Deposition of SiN_x:H thin films by the electron cyclotron resonance and its application to Al/SiN_x:H/Si structures

S. Garcia, I. Martil,[a] and G. Gonzalez Diaz
Departamento Electricidad y Electronica, Facultad Fisicas, Universidad Complutense de Madrid, 28040 Madrid, Spain

E. Castan and S. Dueñas
Departamento Electricidad y Electronica, Facultad Ciencias, Universidad de Valladolid, 47011 Valladolid, Spain

M. Fernandez
Instituto de Ciencia de Materiales, Cantoblanco, 28049 Madrid, Spain

(Received 28 March 1997; accepted for publication 15 September 1997)

We have analyzed the electrical properties and bonding characteristics of SiN_x:H thin films deposited at 200 °C by the electron cyclotron resonance plasma method. The films show the presence of hydrogen bonded to silicon (at the films with the ratio N/Si$<$1.33) or to nitrogen (for films where the ratio N/Si is higher than 1.33). In the films with the N/Si ratio of 1.38, the hydrogen content is 6 at. %. For compositions which are comprised of between N/Si= 1.1 and 1.4, hydrogen concentration remains below 10 at. %. The films with N/Si= 1.38 exhibited the better values of the electrical properties (resistivity, 6×10^{13} Ω cm; and electric breakdown field, 3 MV/cm). We have used these films to make metal-insulator-semiconductor (MIS) devices on n-type silicon wafers. $C-V$ measurements accomplished on the structures indicate that the interface trap density is kept in the range $(3-5)\times10^{11}$ cm^{-2} eV^{-1} for films with the N/Si ratio below 1.38. For films where the N/Si ratio is higher than 1.4, the trap density suddenly increases, following the same trend of the concentration of N–H bonds in the SiN_x:H films. The results are explained on the basis of the model recently reported by Lucovsky [J. Vac. Sci. Technol. B **14**, 2832 (1996)] for the electrical behavior of (oxide–nitride–oxide)/Si structures. The model is additionally supported by deep level transient spectroscopy measurements, that show the presence of silicon dangling bonds at the insulator/semiconductor interface (the so-called P_{bN0} center). The concentration of these centers follows the same trend with the film composition of the interface trap density and, as a consequence, with the concentration of N–H bonds. This result further supports the N–H bonds located at the insulator/semiconductor interface which act as a precursor site to the defect generation of the type •Si≡Si_3, i.e., the P_{bN0} centers. A close relation between interface trap density, P_{bN0} centers and N–H bond density is established. © *1998 American Institute of Physics.*
[S0021-8979(97)03724-9]

I. INTRODUCTION

The electron-cyclotron-resonance plasma method (ECR) has proved to be one of the most suitable deposition procedures to obtain insulator thin films. Device quality SiN_x:H,[1] SiO_2,[2] and SiO_xN_y,[3] have been deposited at a low substrate temperature with this technique.

There are reports on metal-insulator-semiconductor devices (MIS) with different semiconductors in which the insulator was deposited by the ECR plasma method. Structures such as SiN_x/InP,[4] SiN_x/GaAs,[1] and SiN_x/InGaAs (Ref. 5) have been described recently, with good interface characteristics. The good electrical behavior exhibited by these devices was attributed to the "soft" character of the ECR plasma method.

In the field of Si based MIS devices, the use of SiN_x:H films has shown a growing interest. As device dimensions shrink below 0.1 μm in ultralarge scale integrated circuits (ULSI), the thickness of the gate dielectric in field effect transistors (FETs) falls to the 3–4 nm range. In these ultrathin insulators, the incorporation of SiN_x:H interlayers to the standard SiO_2 dielectric film appears to be successful in order to improve gate performance.[6,7] Gate dielectric structures of the type oxide/nitride/oxide have shown excellent characteristics that allow them to be used in ULSI circuits.[8] The analysis of these structures has shown that the presence of N–H bonds at the insulator/semiconductor interface plays a main role in the electrical behavior of the MIS structure.[9] From the data of Refs. 10 and 11, it is suggested that the N–H bonds may act as precursor sites for defect generation at the nitrided-SiO_2/Si interface.

The electrical behavior of the SiN_x:H/Si interface is not as well known as the SiO_2/Si interface. It is argued that the high intrinsic film stress is responsible for a high density of interfacial traps,[12] resulting in poorer structures. Few papers dealing with the electrical characteristics of SiN_x:H/Si structures have been published. The microscopic origin of interfacial defects on these structures is not well known.[13] Indeed, the use of SiN_x:H films deposited by ECR in SiN_x:H/Si MIS devices is scarce.[14,15]

[a]Electronic mail: imartil@eucmax.sim.ucm.es

 0021-8979/98/83(1)/332/7/$15.00 © 1998 American Institute of Physics

Copyright © 1998. All rights reserved.

In view of the increasing interest of SiN_x:H interlayers in gate dielectric structures, in this paper we will present a detailed study of the electrical characteristics of SiN_x:H/Si MIS devices in which the SiN_x:H films are deposited by the ECR plasma method at low temperatures.

The aim of the paper is twofold:

(i) To analyze the properties of the SiN_x:H films in relation to their use in MIS devices. The main emphasis is paid on the atomic bonding arrangement of films and on their electrical properties. These are analyzed by measuring the accumulation zone of $I-V$ characteristics of MIS structures.

(ii) To know details about the electrical characteristics of the SiN_x:H/Si interface, $C-V$ measurements and deep level transient spectroscopy (DLTS) characterizations are conducted on the devices. To the best of our knowledge, this technique is scarcely used to analyze SiN_x:H/Si MIS devices.

II. EXPERIMENT

The deposition system used in this study consists of an Astex 4500 ECR plasma source attached to a deposition chamber of our design. Microwave power (2.45 GHz) was introduced into the source through a coaxial cable and a fused quartz window. N_2 was used to generate the plasma and pure SiH_4 was introduced into the deposition chamber through a gas dispersal ring. The deposition parameters which we chose to deposit the films were the microwave power (50–200 W), and the gases flux ratio N_2/SiH_4 (R, in the following), with values comprised of between 0.5 and 9. Pressure (0.6 mTorr) and substrate temperature (200 °C) were kept constant in all the depositions.[16]

Film properties were analyzed with different techniques. The composition of the films, deposited on Si substrates, was measured by Auger electron spectroscopy (AES). Measurements were carried out in a JEOL JAMP-10S system. The Si (LVV), and N (KLL) transitions were measured. To obtain the bulk composition, samples were sputtered with Ar ions of 2 kV, until a constant value of the Auger signals was reached. Then, quantitative results were obtained with the corresponding relative sensitivity factors.[17] To avoid the influence of preferential resputtering effects, we used a reference sample in all the measurements.

Bonding configuration of the films was deduced with infrared absorption characterization. Measurements were obtained with a Fourier transform infrared (FTIR) Nicolet 5PC spectrometer in the midinfrared region ($400-4000\ cm^{-1}$), for films deposited on high-resistivity (80 Ω cm) Si substrates, both sides polished. The hydrogen concentration of the films, [H], was calculated from the Si–H and N–H stretching absorption peaks using the method of Lanford and Rand.[18] The spin density of the films was determined by electron paramagnetic resonance (EPR) measurements, using a Bruker ESP 300E X-band spectrometer.

MIS devices were obtained as follows: the substrates used were n-Si (5 Ω cm, ⟨100⟩ orientation), in which we have previously deposited Al back electrodes by thermal evaporation. We cleaned the wafers with organic solvents. After this, the native oxide was stripped with a H_2O:HF (10:1) solution during 30 s, followed by a 3 min rinse in deionized water.[19] 500 Å thick SiN_x:H film was then deposited on the top of the Si surface. Finally, Al dots were evaporated through a shadow mask to define square electrodes of $1.2\times10^{-3}\ cm^2$. A postdeposition annealing was done at 400 °C during 20 min in a N_2 atmosphere.

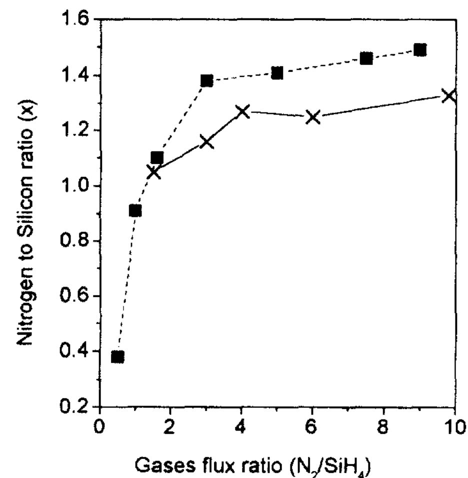

FIG. 1. Nitrogen to silicon ratio for the films as a function of the gas flux ratio (R) (■). Also shown, the results of Ref. 1 for ECR films deposited at 500 °C (×).

The electrical properties of the films (resistivity, ρ, and breakdown field, E_B) were obtained by measuring the $I-V$ characteristics of the MIS structures. The resistivity was obtained at an electric field of 2 MV/cm.[20] The value of E_B was obtained at the field at which the MIS current reaches 1 $\mu A/cm^2$.[21]

$C-V$ characteristics [quasistatic (QS) and high frequency (HF) curves], were obtained with a Keithley Model 82 system. The analysis of the $C-V$ data was done following the procedure described by Nicollian and Brews.[22]

DLTS measurements were performed using a 1 MHz Boonton 72B capacitance meter and an HP 54501A digital oscilloscope to record the complete capacitance transients. The quiescent bias voltage was introduced by a Keithley 617 programmable electrometer, and the filling pulses were introduced by an HP 214B pulse generator. Samples were cooled in darkness from room temperature to 100 K at zero bias in an Oxford DN1710 cryostat.

The interface-state profiles were obtained by saturating pulse DLTS.[23,24] The bias voltage was chosen so that the MIS capacitor was just at the limit between depletion and weak inversion. A 10-ms wide pulse high enough to drive the capacitors into accumulation was applied in order to fill all interface traps. Information on the traps was obtained by analyzing the capacitance transient that results as the traps empty, i.e., return to equilibrium.

III. RESULTS AND DISCUSSION

The main deposition parameter that determines the film properties was the gas flux ratio, R.[25] In Fig. 1, we show the N/Si ratio of films (in the following, x) as a function of R, for films deposited at 100 W (the same power that we chose to obtain the MIS structures). As a comparison, we present in the same figure the results of Park,[1] for films of SiN_x:H

Copyright © 1998. All rights reserved.

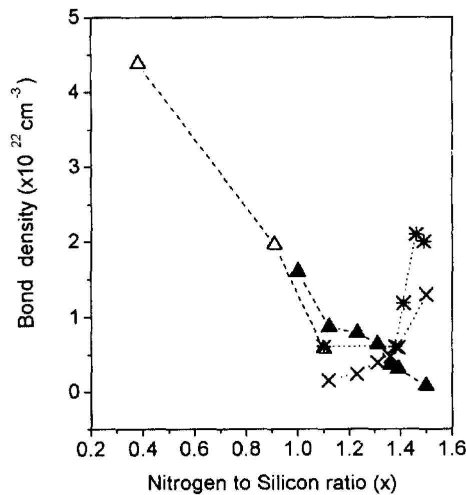

FIG. 2. Concentration of Si–H (△) and N–H (∗) bonds of the films as a function of film composition, x. We also present the concentration of Si–H bonds (▲) and the N–H bonds (×) for films of SiN_x:H deposited by PECVD at 250 °C (Ref. 26).

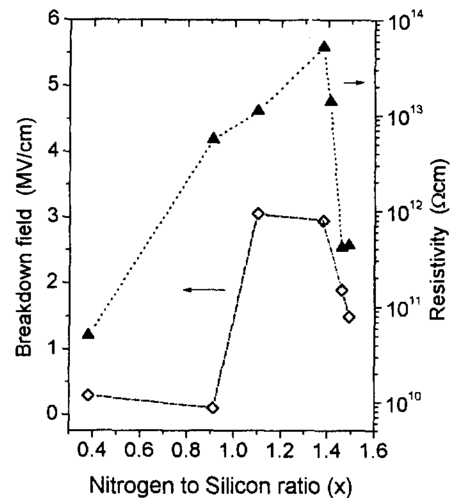

FIG. 3. Electric breakdown field (◇) and resistivity of films (▲) as a function of x.

obtained by ECR and using the same precursor gases as those utilized in this study. The main difference is in relation with the deposition temperature [200 °C for our films, 500 °C for the data of Park[1]]. From the figure, it can be deduced that we obtained SiN_x:H films with a wide range of compositions, with values of x ranging from $x \leqslant 0.91$ (at $R \leqslant 3$), to $x \geqslant 1.45$ (at $R \geqslant 7.5$). The trend is similar to the data of Park *et al.*,[1] with slight differences on the absolute values.

In Fig. 2, we present the concentration of Si–H and N–H bonds of the films, as a function of x. Si–H bonds are dominant in Si-rich films, whereas N–H bonds are observed in N-rich films. This trend is well known to hold in SiN_x:H films deposited by plasma methods.[26] The comparison with other results is difficult, because of the different precursor gases, deposition temperature, and other process parameters used in the deposition. These parameters have a main influence on the bonding arrangement and on the total amount of hydrogen of the films. Anyway, we have included in Fig. 2 the data of Parsons,[26] for PECVD films that were deposited with the same precursor gases and very similar deposition temperature (250 °C) to those reported here. The transition from films dominated by Si–H bonds to those dominated by N–H occurs at a film composition of $x \sim 1.3$ for both set of data. Depending on the plasma reactor and on the deposition conditions, the results may vary in a relatively wide range.[27] Our data indicate that for compositions ranging from $x = 1.1$ to $x = 1.4$, the total amount of bonded hydrogen (deduced from the concentrations of Si–H and N–H bonds) remains around 10 at. % and, at the film composition with $x = 1.38$, this amount is as low as 6 at. %. This result is among the better ones reported in the literature for SiN_x:H films deposited for any plasma method at low deposition temperature.

The $I-V$ characteristic of the MIS structures are similar to those showed in Ref. 28 for films also deposited by ECR. We have not accomplished a detailed analysis of these characteristics being used by the data in this study to obtain the value of the resistivity, as we have explained in Sec. II.

In Fig. 3, we present the values of the electric breakdown field, E_B, and the film resistivity, ρ, as a function of film composition, x. The maximum of both parameters is obtained at film compositions that range from $x = 1.1$ to $x = 1.41$. On the other hand, in films with composition far from this range, both E_B and ρ values fall down. At the composition with $x = 1.38$, the values of E_B and ρ are 3 MV/cm and 6×10^{13} Ω cm, respectively. The values of the resistivity indicates that the films are not "perfect" insulators. The presence of defects of a diverse nature may account for the values of ρ presented in Fig. 3 that are lower than those obtained in pyrolitic CVD silicon nitride but similar to the values reported in films obtained with plasma CVD techniques in which the deposition temperature was higher than that used in this study.[15] We will subsequently analyze the defects present in the films.

Figures 2 and 3 indicate that in the films that show poor values of the electrical parameters, i.e., in the films with the parameter x lower than 1.1 or higher than 1.41, [H] is high. The relation between E_B and the presence of hydrogen in the films was fairly suggested by Hasegawa[29] for films deposited by PECVD; however an unambiguous relation never has been established. The stress of the films, directly related with the presence/absence of hydrogen, may play some specific role in the understanding of breakdown properties of SiN_x:H films.

In relation with the film resistivity, in Fig. 4 we present the dependence of this parameter and also the dependence of [H] with the composition, x. As in the case of E_B, a close relation between both parameters seem to hold. Although some papers have been published trying to explain the relation between ρ and [H],[20] a definitive model has not yet been established, as in the case of the relation E_B-[H].

The main conclusion found from Figs. 3 and 4 is that in a relatively wide range of film compositions (from $x = 1.1$ to $x = 1.4$), we may obtain SiN_x:H films with electrical properties similar to those obtained with plasma deposition meth-

Copyright © 1998. All rights reserved.

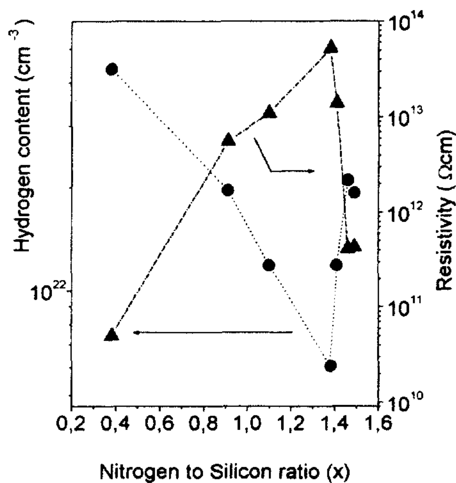

FIG. 4. Resistivity (▲) and hydrogen content (●) as a function of x.

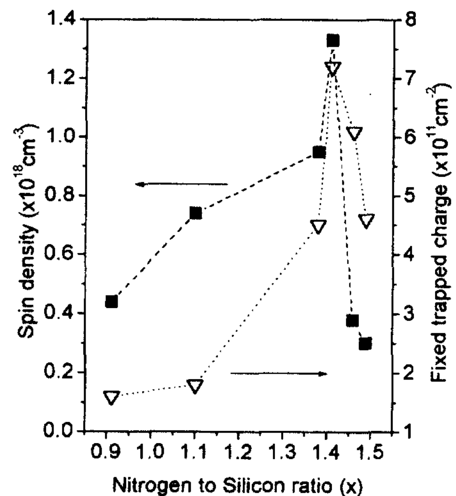

FIG. 6. Fixed trapped charge at the insulator (▽) and spin density (■), as a function of x.

ods which use higher substrate temperatures than the value used in this study.

In Fig. 5, we present the $C-V$ characteristic (both QS and HF curves) for a MIS in which the film composition is $x=1.38$. The dip observed in the QS curve is a clear indication of the high quality of the SiN_x:H/Si interface.

From the data of the flatband voltage, we have deduced the values of the fixed trapped charge at the insulator (Q_i). This was always positive, as it is commonly reported in SiN_x:H films.[7] In Fig. 6, we have plotted the values of Q_i and the spin density of the bulk of the films, deduced from EPR measurements,[30] as a function of the composition, x. It is worth noting that EPR measurement accounts for the presence of defects that are paramagnetically active both in the bulk of the insulator and also at the interface with the Si substrate. Since our films are defective, the contribution to the EPR signal coming from defects located at the SiN_x:H/Si interface should be a small fraction of the total measurement signal. We then conclude that the EPR characterization allows us to obtain the density of defects (paramagnetically active) present in the bulk of the insulator. Only if the insulator is free of defects (for instance, thermally grown SiO_2 onto Si), the EPR characterization can be used with care to obtain information concerning the presence of defects at the insulator/semiconductor interface.[31]

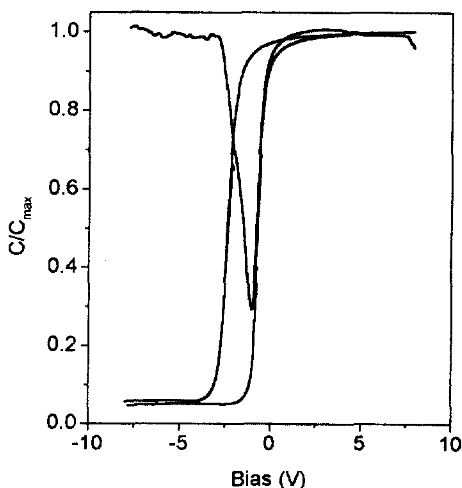

FIG. 5. Quasistatic and high frequency $C-V$ curves for a structure with an insulator with $x=1.38$.

The trend with x shown by both the spin density and Q_i is very similar for both parameters. The behavior of the spin density was already explained elsewhere.[30] The origin of such a defect is the well-known Si dangling bond ($\bullet Si\equiv Si_3$), present in the bulk of the insulator. As the film composition changes from $x=0.91$ to $x=1.38$ the Si dangling bonds will be easily formed by breaking Si–Si bonds.[27] At compositions around $x=1.4$, the spin density and Q_i reach their maximum value. Notice that at this composition, the presence of hydrogen at the films is minimum. Due to this fact, the number of unpassivated Si dangling bonds should reach their maximum concentration, as shown in Fig. 6. Once the films become N rich, there is a sharp increase in the presence of N–H bonds (see Fig. 2). These bonds induce a decrease in the concentration of Si dangling bonds, as was suggested by Hasegawa.[27] This fact explains the sharp decrease observed in Fig. 6 for the spin density. The fact that Q_i follows the same dependence with x of the spin density, allows us to tentatively identify the microscopic origin of the fixed trapped charge Q_i, with the Si dangling bonds. However, some caution should be taken in this assignment. The technique EPR gives a direct measurement of defects that are paramagnetically active. Other type of defects not detectable by EPR like neutral defects, dangling bonds with two unsaturated bonds, can also contribute to Q_i. From Fig. 6, it seems that the main contribution to Q_i comes from the Si dangling bonds.

In Fig. 7, we present the hysteresis (ΔV_{hys}) of the curve $C-V$ as a function of the film composition, x. As known, films with low values of x present high values for this parameter, whereas films with x higher than 1.3 usually exhibit lower ones.[21]

Copyright © 1998. All rights reserved.

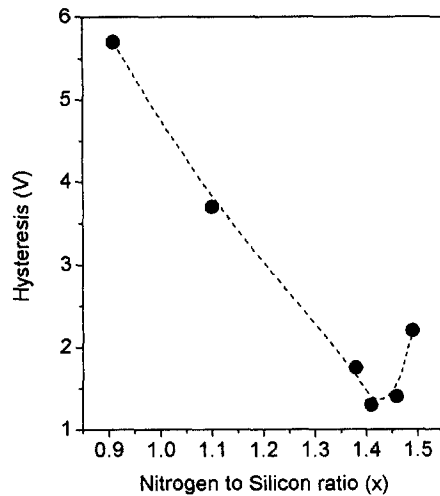

FIG. 7. Voltage hysteresis for the MIS analyzed, as a function of film composition, x.

On the other hand, we have deduced the distribution of the interface trap density within the forbidden gap (D_{it}) by means of $C-V$ and DLTS measurements. The distribution of D_{it} is obtained from the curves $C-V$ by means of the equation:[22]

$$C_{it}=qD_{it}=(1/C_{\mathrm{LF}}-1/C_1)^{-1}-(1/C_{\mathrm{HF}}-1/C_1)^{-1}, \quad (1)$$

where $C_{\mathrm{LF}},C_{\mathrm{HF}}$ are the values of the capacitance (per unit of area) of the MIS at low and high frequency, respectively, and C_1 is the capacitance of the insulator. We show in Fig. 8 the result of this analysis for the device in which the composition of the insulator is $x=1.38$, i.e., for the structure presented in Fig. 5. The minimum value of D_{it} appears around 0.15 eV above the midgap, similar to the results reported by Sitbon[15] for SiN_x:H/Si devices in which the insulator was deposited by distributed ECR. From the figure, it can be seen that the density of traps remains below 10^{12} $\mathrm{cm}^{-2}\,\mathrm{eV}^{-1}$ in a wide range of energies. This further supports the good quality of the interface.

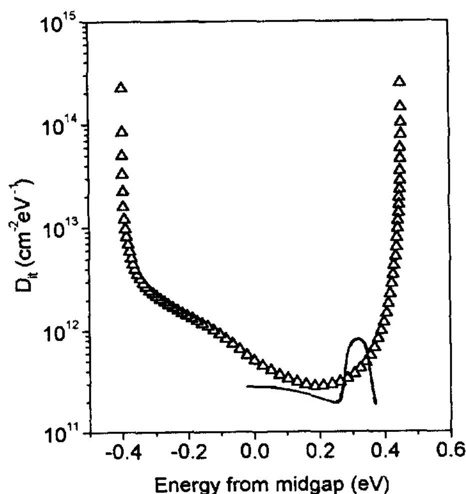

FIG. 8. Interface trap distribution within the forbidden gap deduced from the $C-V$ data (△), and from the DLTS measurements (---). The film composition is $x=1.38$.

For the calculation of D_{it} from DLTS spectra, the following expressions were used:[22]

$$N_{SS}=\frac{\epsilon_s N_D}{KT}\,\frac{C_I[C(t_2)-C(t_1)]}{[C(t_1)]^3}\,\frac{1}{\ln(t_2/t_1)} \quad (2)$$

$$E=E_C-KT\,\ln\,\sigma_n(E)v_{th}N_C\,\frac{t_2-t_1}{\ln(t_2/t_1)}, \quad (3)$$

where $C(t)$ is the capacitance at time t, C_I is the capacitance of the insulator, σ_n is the interface state capture cross section, v_{th} is the thermal velocity of electrons, and N_c is the effective density of states of the conduction band. An energy-independent capture cross-section value of $\sigma_n=1\times10^{-14}$ cm^{-2} was used in the calculation, which is typically found in Si-MIS structures.[22,32]

Figure 8 also shows that the interface states profile of the device where $x=1.38$ (i.e., the device showed in Fig. 5), is obtained by DLTS. We can observe the presence of a maximum located at about 0.3 eV above the midgap (0.25 eV below the edge of the conduction band). This peak has been found in all the samples of our study, and it can be identified with the $P_{b\mathrm{N}0}$ defect. This defect was reported by Stesmans[13] as the $\bullet\mathrm{Si}\equiv\mathrm{Si}_3$ defect in $\mathrm{Si/Si_3N_4}$ interface, i.e., the surface Si dangling bond (also described in this paper as the unpaired hybrid pointing out the Si surface). The origin of this defect is the same as the origin of the P_{b0} defect in the $\mathrm{Si/SiO_2}$ interface.[33] The concentration of $P_{b\mathrm{N}0}$ centers present at the SiN_x:H/Si interface is then deduced from the data of Fig. 8 in a straightforward way.

In comparing the interface state profiles obtained by $C-V$ and DLTS, we can see that the shape of the distribution is different, though both techniques provide values for the interface trap density of the same order of magnitude. Differences between $C-V$ and DLTS measurements can be accounted for by the presence of slow states at the insulator/semiconductor interface, i.e., defects that are somewhat distributed away from the interface into the insulator. When the interface states are distributed in such a way, the electron emission and capture processes involve both thermal excitation and tunneling, producing a broad time constant dispersion, thus affecting the interface trap distribution obtained by $C-V$ and DLTS measurements in different ways,[34,35] thus justifying the shape of trap distribution of Fig. 8. The hysteresis observed in $C-V$ curves (Fig. 7) should be in relation with the above-mentioned processes. To further confirm the presence of such slow states, we have performed conductance transient measurements of the devices. These transients appear in a wide temperature range (200 K to room temperature), and their shape is very dependent on the measurement frequency. Elsewhere we have explained[36] that these transients in terms of tunneling assisted emission and capture processes of electrons between the semiconductor conduction band and the interface states located far away from the interface up to distances of at least 30 Å. This further confirms the previous discussion.

Copyright © 1998. All rights reserved.

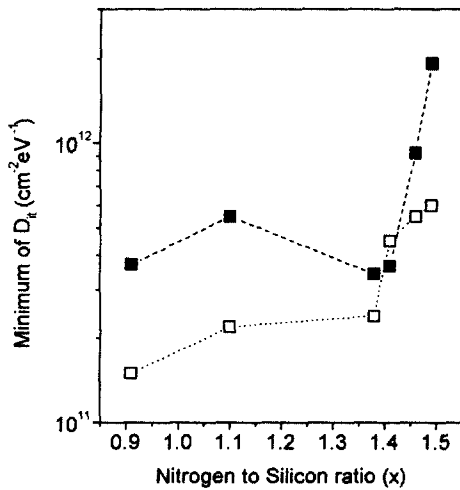

FIG. 9. Minimum value of D_{it} as a function of x, deduced from $C-V$ curves (■), and from DLTS (□).

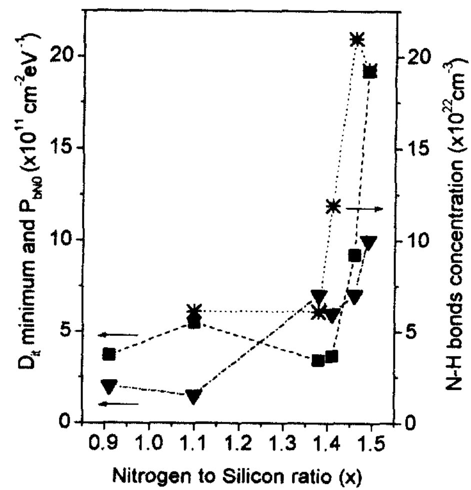

FIG. 10. Minimum value of D_{it} [deduced from $C-V$ characterization (■)], concentration of P_{bN0} centers (▼) and concentration of N–H bonds (*), as a function of film composition, x.

In Fig. 9, we present the minimum of D_{it} (deduced from $C-V$ measurements) as a function of film composition, and the values of this parameter obtained from the DLTS at the same energy at which the minimum of the $C-V$ curve appears. The trend shown by the two sets of data is coincident. For film compositions lower than $x=1.38$, the minimum of D_{it} is a slight function of x. For this range of compositions, the values of D_{it} are below 5×10^{11} cm^{-2} eV^{-1} and the typical value is $(2-3)\times10^{11}$ cm^{-2} eV^{-1}. This is among the lower values described for the SiN_x:H/Si interface. The devices with SiN_x:H films in which $x>1.4$, exhibit a sharp increase in the values of D_{it}, i.e., the interface becomes more defective.

The results we present in Fig. 9 can be understood on the basis of the role that N–H bonds play in the behavior of the interface between SiN_x:H and Si, according to the model of Lucovsky.[10,11] Although this model was developed to explain the electrical characteristics of (oxide–nitride–oxide)/Si interfaces,[8] we think that their main conclusions also hold for SiN_x:H/Si devices. In fact, in Fig. 10 we plot the minimum of the interface trap density (deduced from the $C-V$ curves), and the concentration of N–H bonds, as a function of the film composition. We have also plotted in the same figure the concentration of P_{bN0} centers. As was explained in the previous paragraph, this parameter accounts for the number of dangling bonds with the unpaired hybrid pointing out the Si surface, i.e., the number of interface defects of the type $\bullet Si\equiv Si_3$. From Fig. 10, the dependence of the three parameters with the composition is very similar: for compositions below $x\approx1.4$, all of them remain roughly constant. For values of x higher than 1.4, the three increase sharply. Notice that the rise observed in D_{it} and in P_{bN0} parallels the increase of the concentration of N–H bonds.

Following the model of Lucovsky,[10,11] the presence at the SiN_x:H/Si interface of a N–H bond located in the vicinity of a Si–H surface terminated bond, promotes the formation of a $N-H_2$ bond (via the trapping of a hole). This process gives rise to the formation of a dangling bond of the type $\bullet Si\equiv Si_3$, i.e., to the formation of P_{bN0} centers. The dependence of the concentration of these centers with the film composition (Fig. 9) and the close relation between this concentration and the N–H bonds (Fig. 10) seems to confirm this explanation.

From the results of Figs. 7, 9, and 10, we deduce that N–H bonds have the main influence on the electrical characteristics of Al/SiN_x:H/Si MIS capacitors. This influence is different depending on the location of these bonds. When they are in the bulk of the insulator, they promote the decrease of Si dangling bonds and the decrease of the fixed trapped charge at the insulator, Q_i. On the other hand, N–H bonds at the interface with the semiconductor act as a precursor site to defect generation of the type of Si dangling bonds. As a consequence, the interface is more defective as the concentration of the N–H bonds increases.

As a final comment, we wish to state that one year after we fabricated the structures, their behavior remains essentially unchanged, which proves the quality of the procedure we followed to obtain them.

IV. CONCLUSIONS

We have deposited thin films of SiN_x:H by the ECR plasma method at a deposition temperature of 200 °C. The films present a low content of bonded hydrogen. In the range of compositions from $x=1.1$ to $x=1.4$, the parameter is around 10 at. %, and at film composition $x=1.38$, is 6 at. %. This qualifies the films to be used as the gate dielectric in MIS devices. The electrical properties of films (resistivity and electric breakdown field) are strongly in influenced by the film composition and by the hydrogen content. The best values attained for these two parameters are obtained for films with $x=1.38$, in which the content of hydrogen is minimum.

From the $C-V$ characterization of the devices, we deduced that the fixed trapped charge at the insulator is dominated by the bonding arrangement of the films. The films that present significant amounts of N-H bonds, have low values

Copyright © 1998. All rights reserved.

of fixed trapped charge. Also, the density of bulk dangling bonds deduced from EPR measurements follows the trend of the trapped charged with the composition of the insulator. These facts seem to indicate that the presence of N–H bonds are the main influence in the reduction of the charge of the insulator bulk.

The interface trap distribution of the devices, deduced from $C-V$ and DLTS measurements, showed a similar behavior with small differences coming from the different procedures of measurement. These differences are explained taking into account both the energy and the spatial distribution of the interface states, i.e., taking into account the presence of slow states at the insulator/semiconductor interface. We deduced a close relation among the minimum of the interface trap density, the concentration of P_{bN0} centers and the concentration of N–H bonds in the films. These bonds, located at the SiN_x:H/Si interface, act as precursor sites to defect generation of the type $\bullet Si \equiv Si_3$, i.e., the center P_{bN0}. These sets of results are in close agreement with the model of Lucovsky.[10,11] Also, we conclude the different influence that N–H bonds have, depending on if we consider their influence in the bulk of the insulator or at the interface with the semiconductor.

The results we have presented here could be a significant advance in the comprehension of the behavior of SiN_x:H/Si devices.

ACKNOWLEDGMENTS

The authors would like to thank E. Iborra for the facilities of the infrared characterization of the films. This work was partially supported by the Spanish Government (CICYT), under Grant TIC 93/0175.

[1] D. G. Park, M. Tao, D. Li, A. E. Botchkarev, Z. Fan, Z. Wang, S. N. Mohammed, A. Rockett, J. R. Abelson, and H. Morkoc, J. Vac. Sci. Technol. B **14**, 2674 (1996).
[2] K. H. Chew, J. Chen, R. C. Woods, and J. L. Sohet, J. Vac. Sci. Technol. A **13**, 2483 (1995).
[3] R. I. Hegde, P. J. Tobin, K. G. Reid, B. Maiti, and S. A. Ajuria, Appl. Phys. Lett. **66**, 2882 (1995).
[4] A. Kapila, X. Si, and V. Malhotra, Appl. Phys. Lett. **62**, 2259 (1993).
[5] P. J. M. Permiter and J. G. Swanson, J. Electron. Mater. **25**, 1506 (1996).
[6] Z. Lu, S. S. He, Y. Ma, and G. Lucovsky, J. Non-Cryst. Solids **187**, 340 (1995).
[7] Y. Ma, T. Yasuda, and G. Lucovsky, J. Vac. Sci. Technol. A **11**, 952 (1993).
[8] Y. Ma, T. Yasuda, and G. Lucovsky, Appl. Phys. Lett. **64**, 2226 (1994).
[9] D. R. Lee, G. Lucovsky, M. S. Denker, and C. Magee, J. Vac. Sci. Technol. A **13**, 1671 (1995).
[10] Z. Ying, G. Lucovsky, and J. L. Whitten, J. Vac. Sci. Technol. B **13**, 1613 (1995).
[11] G. Lucovsky, Z. Ying, and D. R. Lee, J. Vac. Sci. Technol. B **14**, 2832 (1996).
[12] R. C. Budhani, R. F. Bunshah, and P. A. Finn, Appl. Phys. Lett. **52**, 284 (1988).
[13] A. Stesmans, Semicond. Sci. Technol. **4**, 1000 (1989).
[14] D. Landheer, J. A. Bardwell, I. Spraule, J. Scott-Thomas, W. Kwok, and W. M. Lau, Can. J. Phys. **70**, 795 (1992).
[15] S. Sitbon, M. C. Hugon, B. Agius, F. Abel, J. L. Courant, and M. Puech, J. Vac. Sci. Technol. A **13**, 2900 (1995).
[16] S. Garcia, J. M. Martin, I. Martil, M. Fernandez, and G. Gonzalez Diaz, Philos. Mag. B **73**, 487 (1996).
[17] *Handbook of Auger Electron Spectroscopy*, 2nd ed. (Physical Electronics Industries, Eden Prairie, MN, 1976).
[18] W. A. Lanford and M. J. Rand, J. Appl. Phys. **49**, 2473 (1978).
[19] L. J. Huang and K. M. Lau, Appl. Phys. Lett. **60**, 1108 (1992).
[20] M. Maeda and Y. Arita, J. Appl. Phys. **53**, 6852 (1982).
[21] W. S. Lau, S. J. Fonash, and J. Kanicki, J. Appl. Phys. **66**, 2765 (1989).
[22] E. H. Nicollian and J. R. Brews, *MOS Physics and Technology* (Wiley, New York, 1982).
[23] D. V. Lang, J. Appl. Phys. **45**, 3023 (1974).
[24] M. Schulz and N. M. Johnson, Appl. Phys. Lett. **31**, 622 (1977).
[25] S. Garcia, J. M. Martin, M. Fernandez, I. Martil, E. Iborra, and G. Gonzalez Diaz, J. Non-Cryst. Solids **187**, 329 (1995).
[26] G. N. Parsons, J. H. Sank, and J. Batey, J. Appl. Phys. **70**, 1553 (1991).
[27] S. Hasegawa, Y. Amano, T. Inokuma, and Y. Kurata, J. Appl. Phys. **72**, 5676 (1992); S. Hasegawa, M. Matsuda, and Y. Kurata, Appl. Phys. Lett. **58**, 741 (1991).
[28] Y. C. Jean, H. Y. Lee, and S. K. Jao, J. Appl. Phys. **75**, 979 (1994).
[29] S. Hasegawa, Y. Amano, T. Inokuma, and Y. Kurata, J. Appl. Phys. **75**, 1493 (1994).
[30] S. Garcia, D. Bravo, M. Fernandez, I. Martil, and G. Gonzalez Diaz, Appl. Phys. Lett. **67**, 3263 (1995).
[31] E. H. Poindexter, G. J. Gerardi, M. E. Bueckel, P. J. Caplan, M. M. Johnson, and D. K. Biegelsen, J. Appl. Phys. **56**, 2844 (1984).
[32] Y. Yamasaki, M. Ooshida, and T. Sugano, Jpn. J. Appl. Phys. **18**, 113 (1979).
[33] R. Helms and E. H. Poindexter, Rep. Prog. Phys. **57**, 791 (1994).
[34] T. Hashizume, H. Hasegawa, R. Riemenschneider, and H. L. Hartnagel, Jpn. J. Appl. Phys., Part 1 **33**, 727 (1994).
[35] H. Hasegawa, M. Akazawa, H. Ishii, A. Uraie, H. Iwadate, and E. Ohue, J. Vac. Sci. Technol. B **8**, 867 (1990).
[36] S. Dueñas, R. Pelaez, E. Castan, R. Pinacho, L. Quintanilla, J. Barbolla, I. Martil, and G. Gonzalez Diaz, Appl. Phys. Lett. **71**, 826 (1997).

Copyright © 1998. All rights reserved.